Ionics (2023) 29:539–547
https://doi.org/10.1007/s11581-022-04847-2

ORIGINAL PAPER

Preparation and properties of NiAl-LDH@S@RGO composite–electrode materials

Hong-Xia Jing[1] · Xu Wang[1] · Na Li[1] · Yan-Lin Gao[1] · Wang-Jun Pei[2]

Received: 11 August 2021 / Revised: 6 November 2022 / Accepted: 30 November 2022 / Published online: 13 December 2022

Abstract

The key challenge of supercapacitors with high power density and good cycle stability is to reasonably design high-performance electrode materials. Therefore, NiAl duble metal hydroxide@sulfide@graphene (NiAl-LDH@S@RGO) composite was prepared by two-step method. The electrochemical properties were characterized by an electrochemical workstation. Compared with the NiAl-LDH (1000.2F/g), the specific capacitance of the composite is nearly doubled due to partial vulcanization and graphene loading. When NiAl-LDH is dispersed in 0.2 mol/L Na_2S, the ratio of load graphene is 30%; the discharge time is 853.2 s; its specific capacitance are up to 1996 $F{\cdot}g^{-1}$ and 1451.4 $F{\cdot}g^{-1}$ at the current density of 1 $A{\cdot}g^{-1}$ and 10 $A{\cdot}g^{-1}$, respectively. After 5000 cycles, it has a capacitance retention ratio of nearly 69%, indicating that the cycling stability of the composite is good. It is concluded that the electrochemical performance of NiAl-LDH@S@RGO was significantly improved by vulcanization and graphene loading.

Keywords Electrode material · NiAl-LDH@S@RGO · Specific capacitance · Discharge time

Introduction

In recent years, with the rapid development of the global economy, fossil fuel consumption, and environmental pollution problems have become increasingly serious [1, 2]. Therefore, there is an urgent need to develop efficient, environmentally friendly and sustainable new energy sources to solve the energy crisis. Supercapacitor (SC) has attracted more and more attention as a new type of energy conversion and storage device for environment sustainable development [3, 4]. It is a new type of capacitor between a conventional battery and a secondary battery [5] and has higher power density than a secondary battery. In addition, SC has safety and environmental protection, excellent charge and discharge performance, good cycle stability [6], etc. Therefore, it can be widely used in electric vehicles, portable electronic equipment, and other fields [7, 8]. However, the low energy density of SC limits its further application [9]. Development of high-performance electroactive materials is the key to increase the energy density of SC.

According to the charge storage mechanism, the SC can be divided into electric double-layer capacitor and pseudo-capacitor [10]. The pseudo-capacitor has a higher capacitance value than that of electric double-layer capacitor, which because that the store charge of pseudo-capacitor is based on a rapid redox reversible reaction on the surface of the electrode material [11, 12].

Transition metal sulfides have higher electrical conductivity. Graphene has a large specific surface area to provide a richer active site for the composite, which provides a faster transmission channel for electrons in the nanosheet, thereby achieving the purpose of improving electrochemical performance. Transition metal double hydroxides (LDH, such as $Ni(OH)_2$, $Co(OH)_2$) have ultra-high theoretical specific capacitance, high redox activity, simple preparation technology, and environment friendly [13]. However, LDH nanosheets are easy to stack together, resulting in insufficient utilization of their active sites, and their conductivity is poor, which limits their further application as electrode materials [14]. Therefore, the electrochemical performance of LDH can be further improved by combining with conductive material [15]. Wang [16] prepared NiAlLDHs@graphene composites by hydrothermal

✉ Hong-Xia Jing
jhx820215@126.com

[1] Department of Chemistry, School of Science, North University of China, Taiyuan 030051, China

[2] Jinxi Industries Group, Taiyuan 030027, China

method. The results show that NiAl-LDHs deposit on the surface of graphene to form a composite after the addition of precipitant (NaOH), the aggregation of LDH and graphene nanosheets was effectively prevented, and the supercapacitor performance was enhanced. Yang [17] prepared a nickel–cobalt layered double hydroxide (NiCo-LDH)@graphene nanosheet with a thickness of 1.7–1.8 nm. When the current density is 1 A/g, the NiCo-LDH-G electrode provides a specific capacitance of up to 1450 F/g, higher than NiCo-OH (932 F/g) specific capacitance, and achieves a 68% capacitance retention ratio, superior to other previously reported NiCo-hydroxide materials. Cha [18] synthesized a stable core–shell structure cobalt sulfide/cobalt aluminum hydroxide nanosheet (LDH-S) through a two-step method. The LDH-S electrode exhibits higher electrochemical performance in terms of specific capacitance and rate performance. Li [19] prepared NiMn-LDH@RGO high-performance electrodes. RGO serves as the second electron collector, which promotes rapid charge transfer and improves electrochemical reaction kinetics. Niu [20] fabricated high-performance supercapacitor materials (a-GNS@NiAl) by in situ growth of NiAl-layered double hydroxide (NiAl-LDH) nanosheets on well-activated graphene nanosheets (a-GNS)-LDH), with large BET surface area and excellent electrical conductivity. These results indicate that LDH can be used to improve its electrochemical performance and conductivity by combining it with a material with better conductivity.

At present, there are few reports about the preparation of LDH@S@RGO composite. The NiAl-LDH@S@RGO composite was prepared by two-step method in this article. First, a layered-NiAl-LDH double hydroxide was synthesized and vulcanized in situ using Na_2S as a sulfur source. Finally, graphene was supported to obtain a final composite. NiAl-LDH@S@RGO was characterized by CV, GCD, EIS.

Experimental

Chemicals

Aluminum nitrate ($Al(NO_3)_3{\cdot}9H_2O$) was purchased in Shanghai Maclean Biochemical Technology Co., Ltd. Nickel nitrate hexahydrate($Ni(NO_3)_2{\cdot}6H_2O$) and anhydrous ethanol (C_2H_5OH) were obtained from Tianjin Kaitong Chemical Reagent Co., Ltd. Sodium sulfide (Na_2S) and potassium hydroxide (KOH) was purchased in Tianjin Shentai Chemical Reagent Co., Ltd. Hexamethylenetetramine($C_6H_{12}N_4$) was purchased in Tianjin Ruijinte Chemical Co., Ltd. Flake graphite powder (1000) was purchased in Qingdao Jinrilai Co., Ltd.

Synthesis of materials

Preparation of NiAl-LDH

About 375 mg (1 mmol) of $Al(NO_3)_3{\cdot}9H_2O$, 582 mg (2 mmol) of $Ni(NO_3)_2{\cdot}6H_2O$, and 1834 mg (13 mmol) of a precipitant (hexamethylenetetramine) were placed in a beaker and fully dissolved in 250 mL of distilled water. The mixture was transferred to a three-necked flask and placed in an oil bath at 95 °C for 5 h. The reaction was centrifuged and washed several times with absolute ethanol and deionized water and dried in a vacuum oven at 60 °C for 12 h to obtain the product.

Preparation of NiAl-LDH@S

The NiAl-LDH was dispersed in 35 mL deionized water, and a certain quality of Na_2S (m(Na_2S): m(NiAl-LDH) = 1:1, 1:2, 1:4, 1:6, 1:8) was added into the above solution. Then the mixed solution was formed by ultrasonic for 2 h. The mixture was transferred to an autoclave and heated to 100 °C in a vacuum oven for 8 h. After the reaction, the product was washed and dried at 60 °C to obtain NiAl-LDH@S compound.

Preparation of NiAl-LDH@S@RGO

Graphene oxide (GO) is prepared by the modified Hummers method [21], and it was reduced by a chemical reduction method (hydrazine hydrate as a reducing agent) to obtain RGO. Then a certain quality of RGO (the mass ratio of RGO is 10%, 20%, 30%, 40%, and 50%, respectively) was added to the Na_2S and NiAl-LDH mixed solution. After ultrasonic dispersion, the mixed solution was transferred to an autoclave and reacted at 100 °C for 8 h. After the reaction, the NiAl-LDH@S@RGO compound was obtained by centrifugal washing and drying.

Preparation of the electrode

The NiAl-LDH@S@RGO, conductive carbon black, and polytetrafluoroethylene, in which the mass ratio was 8:1:1, were mixed and ground for 3–5 h. After supersonic vibration for 2 h in ethanol, the composite of 3.0–5.0 mg was coated on a foamed nickel sheet, in which the diameter was 14 mm. Then, it was vacuum dried at 60 °C for 12 h. Finally, the electrode sheet was obtained by pressing at a pressure of 10 MPa on a tablet machine.

Material characterization

The phase structure was characterized by D/max-rA X-ray diffractometer (XRD, Nippon Science) using Cu Ka radiation, which the testing voltage and current is 40 kV and

100 mA, respectively. The morphology of the samples was characterized by JEM-1011 projection electron microscope (TEM, Japan Electronics Co., Ltd.). The elemental analysis of products was characterized by energy dispersive X-ray spectroscopy (EDX). The CV (cyclic voltammetry), GCD (galvanostatic charge/discharge), and EIS (electrochemical impedance spectroscopy) of the material were tested by VSP-300 modular electrochemical workstation, which used a three-electrode system. The prepared active material electrode sheet, a carbon rod, and a calomel electrode were used as working electrode, counter electrode, and reference electrode, respectively, and the 6.0 mol/L KOH aqueous solution was used as electrolyte. The cycle life of the supercapacitor was tested by Wuhan blue battery test system.

Results and discussion

Effect of different vulcanization ratio

In order to explore the effect of vulcanization degree on electrochemical properties, different mass sulfur sources were used for vulcanization. As shown in Fig. 1a and b, when the mass ratio of sulfur source to NiAl-LDH is 1:4, its CV has the largest area and longest discharge time. According to the charge and discharge formula $Csp = (I\Delta t)/(m\Delta V)$, the specific capacitance of NiAl-LDH@S is 1329.4 F/g. This may be due to the high stability and fast internal electron transmission speed of NiAl-LDH@S complex obtained by direct in situ vulcanization on NiAl-LDH surface. Furthermore, vulcanization increases the roughness of the material surface, which can effectively increase the contact area of the electrode material and the electrolyte. Thus, it can provide more electrochemical active sites [22]. However, with the increase of sulfur sources, both the CV area and the discharge time are decreased. It may be because that, the excessive sulfide can destroy the LDH stable bilayer structure, so it is unable to provide a large specific surface area and affects the exchangeability of interlayer ions.

Effects of different RGO contents

Figure 2a and b show the CV curve and GCD curve of NiAl-LDH@S loaded with different contents of RGO. As shown in Fig. 2a and b, after compounding RGO, the area contained in its CV curve is higher than that of NiAl-LDH@S, indicating that graphene can effectively improve the electrochemical properties of the material. On the one hand, the on-chip structure formed after compounding RGO is beneficial to the contact between the material and electrolyte. On the other hand, compounding RGO weakens the agglomeration effect of NiAl-LDH@S. In pseudocapacitance reaction, the charge storage generally occurs on the material surface,

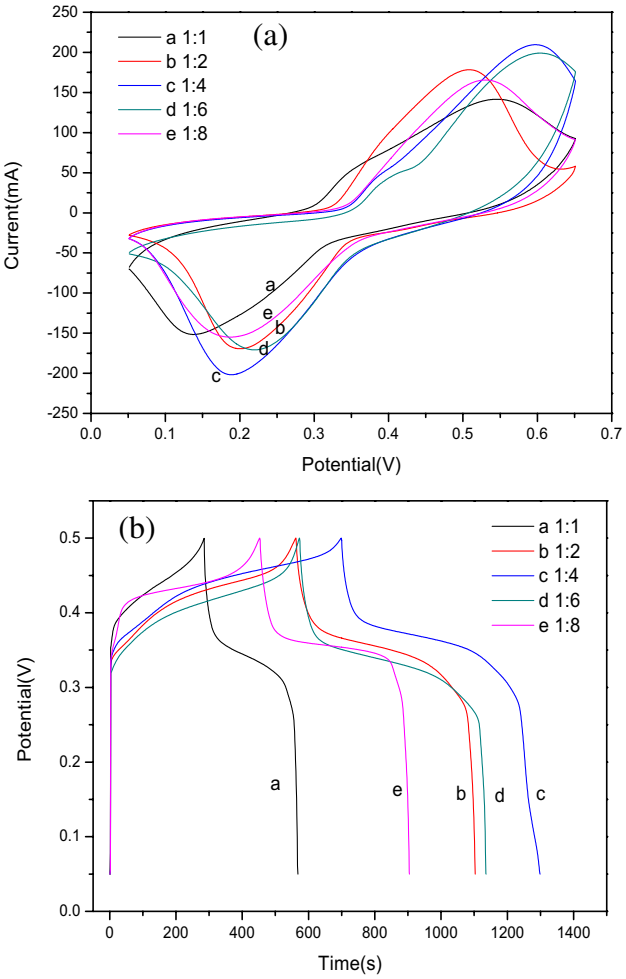

Fig. 1 (**a**) CV curves and (**b**) GCD curves of NiAl-LDH@S with different vulcanization ratios

and the weakening of interlayer agglomeration can provide more ion transfer channels, so as to improve the electrical properties of the material. From Fig. 2a and b, it can also be seen that when the loading amount of RGO is 30%, the NiAl-LDH@S@RGO has the best performance, the specific capacitance value reaches to 1896 F/g.

XRD and Raman characterization

Figure 3 shows the XRD patterns of samples NiAl-LDH, NiAl-LDH@S, and NiAl-LDH@S@RGO. From Fig. 3a, it can be seen that the 2θ values are 11.18 (003), 22.67 (006), 34.91 (012), 61.22 (110), and 65.9 (116), respectively, which accord with that of hexagonal NiAl-LDH (JCPDS, No. 15–0087) [23]. From the spectrum of Fig. 3b, it can be seen that the 2θ value of diffraction peaks is 29.84 (111) and 49.89 (220) which is consistent with the diffraction peaks of Ni_4S_3 (JCPDS, No. 52–1027). It is because the solubility of Ni_4S_3 is much less than that of

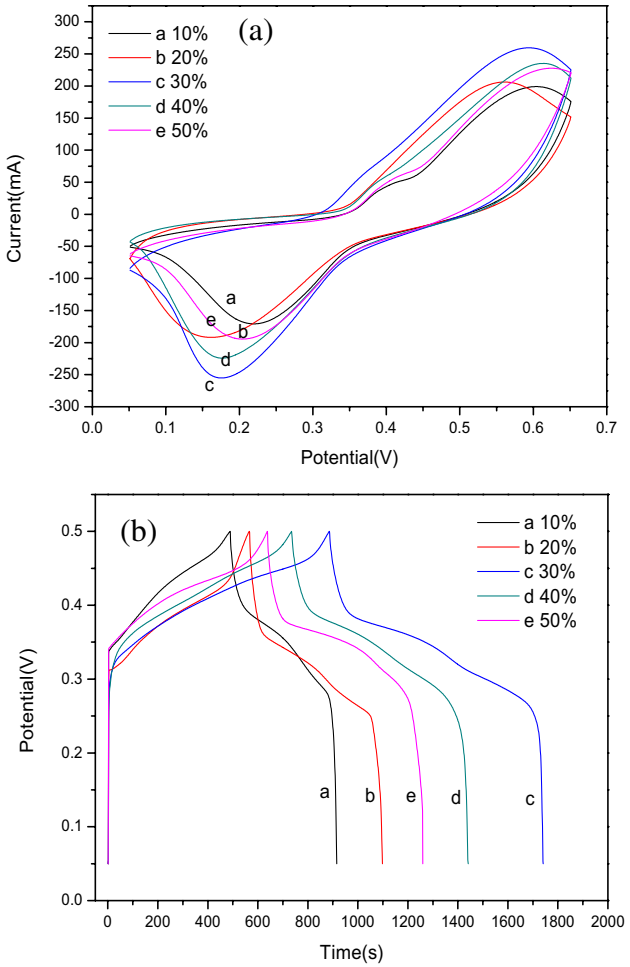

Fig. 2 (**a**) CV curves and (**b**) GCD curves of NiAl-LDH@S@RGO with different RGO contents

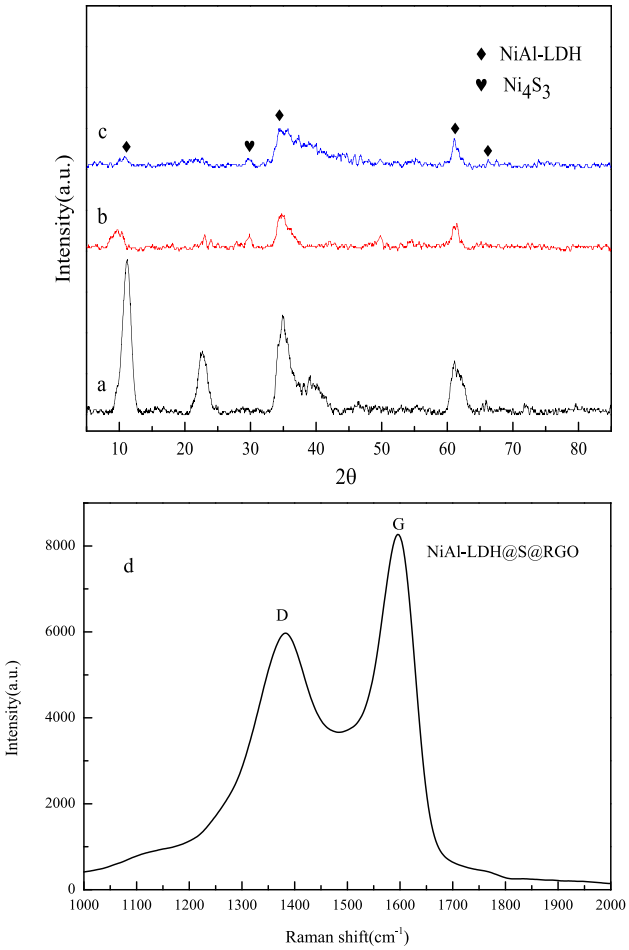

Fig. 3 XRD patterns spectra of samples (**a** NiAl-LDH, **b** NiAl-LDH@S, **c** NiAl-LDH@S@RGO), and **d** Raman spectrum of NiAl-LDH@S@RGO)

nickel hydroxide, but there is no significant difference in solubility between aluminum hydroxide and its sulfide, only Ni_4S_3 was formed. Because of the poor crystallinity of Ni_4S_3, which were adsorbed on the Ni/Al surface, the intensity of diffraction peaks of NiAl-LDH@S is reduced, and the width of diffraction peaks are broadened [24]. This result confirmed that the NiAl-LDH@S was successfully prepared by in situ vulcanization. From the Raman spectrum of NiAl-LDH@S@RGO (Fig. 3d), there are two characteristic peaks at about 1378 and 1587 cm^{-1}, corresponding to the D band and G bands of RGO. It is indicated that the thin NiAl-LDH@S nanoflakes are located on the surface of the graphene nanosheets. However, as can be seen from Fig. 3c, there is no obvious diffraction peak corresponding to RGO. It is because the NiAl-LDH@S nanoflakes, which are located on the surface of the graphene nanosheets, enhance the disordered stacking of graphene nanosheets. The diffraction peaks of NiAl-LDH@S@RGO further diminish due to the amorphous behavior of graphene nanosheets. The diffraction peaks are more broadened. So the degree of amorphization is higher.

EDX analysis

The EDX data of the electrode materials NiAl-LDH, NiAl-LDH@S, and NiAl-LDH@S@RGO are in Fig. 4a, b, and c, respectively. Figure 4a shows the presence of O, Ni, and Al. Figure 4b shows the presence of O, Ni, Al, and S. Figure 4c shows the presence of O, Ni, Al, S, and C. It was confirmed that the products NiAl-LDH, NiAl-LDH@S, and NiAl-LDH@S@RGO were successfully prepared.

TEM analysis

The TEM of samples are shown in Fig. 5. From Fig. 5a, it can be seen that NiAl-LDH is composed of irregular flakes, but most of the NiAl-LDH are aggregated to form dense nanosheets having a large thickness. From Fig. 5b, it can be

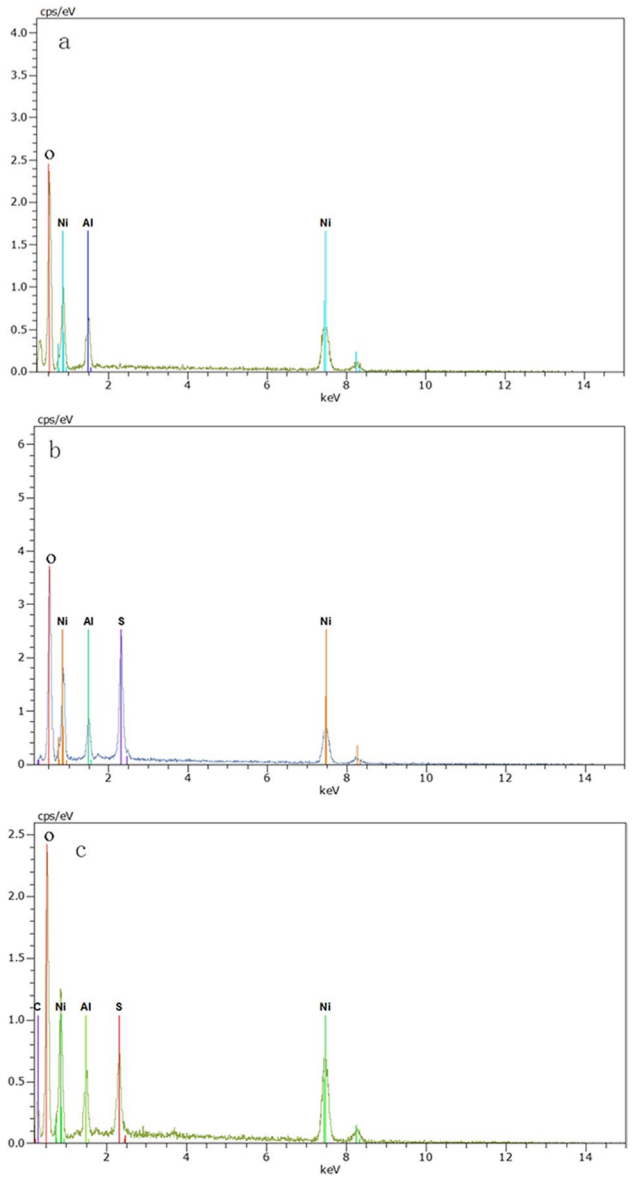

Fig. 4 EDX of samples (**a** NiAl-LDH, **b** NiAl-LDH@S, and **c** NiAl-LDH@S@RGO)

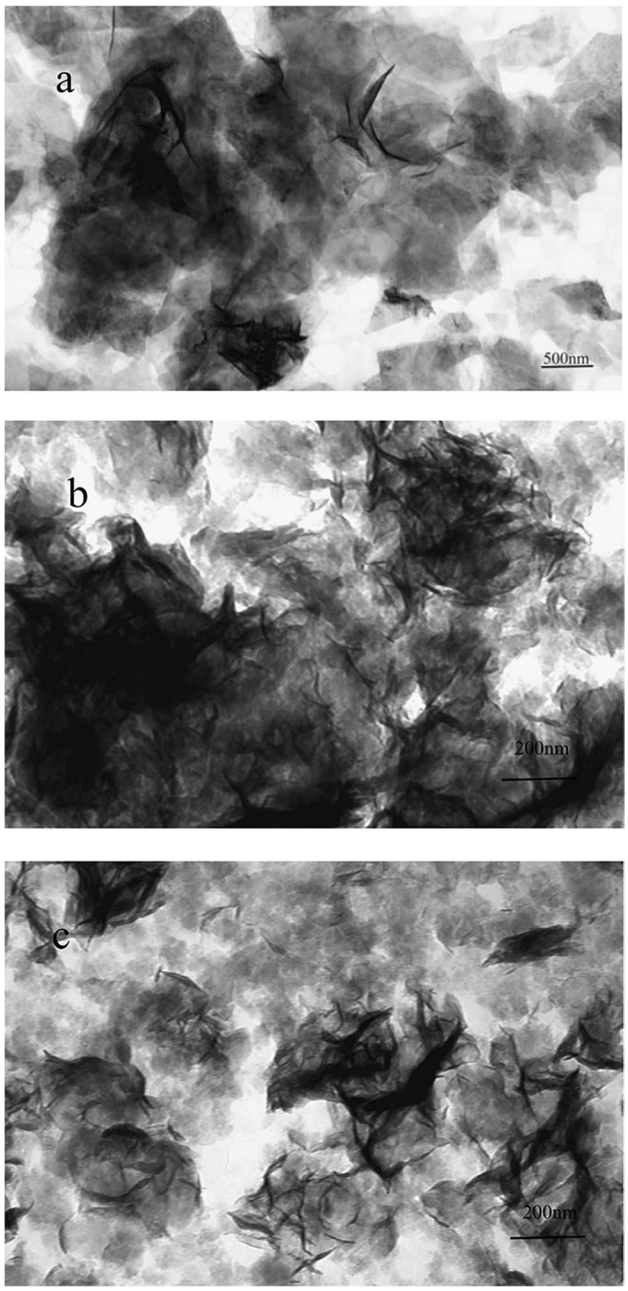

Fig. 5 TEM of samples (**a** NiAl-LDH, **b** NiAl-LDH@S, and **c** NiAl-LDH@S@RGO)

seen that the sulfide retains the basic morphology of LDH, but its surface is rough. This is due to the formation of Ni_4S_3 with poor crystallinity on the NiAl-LDH surface. The rough surface provides more active sites for redox reactions, which is conducive to the improvement of electrical properties. In contrast, after graphene is compounded (Fig. 5c), NiAl-LDH in the composite is better dispersed on the pleated graphene nanosheets, and the aggregation of LDH is effectively prevented, and the electrochemical active sites are effectively increased. It can be seen that NiAl-LDH@S achieves a perfect reproduction with graphene in size and shape. This ultra-thin structure helps the active site to be fully exposed and has higher conductivity.

Electrochemical measurements

The electrochemical properties of the material were characterized by CV. Figure 6a is a CV curve of the NiAl-LDH, NiAl-LDH@S, and NiAl-LDH@S@RGO in a voltage range of 0.05 to 0.65 V and a sweep speed of 20 mV. From the curve shape, the three materials have similar CV curves, which have obvious redox peaks. It indicates that the energy storage mechanism is based on the pseudo capacitance principle, and the reversible redox reaction of Ni^{2+}/Ni^{3+} is on

the surface of the electrode material. The anode peak and the cathode peak are symmetric, indicating high reversibility of the reaction. Meanwhile, it can be seen that the area of the CV curve of NiAl-LDH@S@RGO, NiAl-LDH@S, and NiAl-LDH decreased in turn. The results showed that graphene and sulfide can reduce the agglomeration of NiAl-LDH particles, decrease the resistance during charge transfer, and promote the capacitance performance of the electrode material.

Figure 6b shows the CV curve of NiAl-LDH@S@RGO at different sweep speeds. It can be seen that the shape of the CV curve remains basically unchanged with the increase of the sweep speed, which proves that it has a good rate performance. And as the sweep speed increases, the area of the CV curve also increases, which indicates that the specific capacitance increases with the increase of sweep speed. During this process, the positions of the anode and cathode peaks are slightly offset due to the polarization of the electrodes.

The electrochemical properties of the material were characterized by GCPL. Figure 7a is a GCPL curve of NiAl-LDH, NiAl-LDH@S, and NiAl-LDH@S@RGO at the current density of 1 A/g. From Fig. 7a, it can be seen that the GCPL curve of each sample has a high degree of symmetry and present a non-ideal triangle, indicating that the energy storage mechanism of them is a pseudocapacitance principle, and the reaction has good reversibility. These analysis are well in accord with the CV analysis results. The specific capacitance of NiAl-LDH@S@RGO is up to 1896 F/g, which far exceeds the specific capacitance of NiAl-LDH (1000.2 F/g) and NiAl-LDH@S (1329.4 F/g). Its excellent performance is attributed to the partial vulcanization of NiAl-LDH, which increases the surface roughness. Then it was loaded on the surface of graphene, which effectively improves the re-stacking of RGO and makes full use of

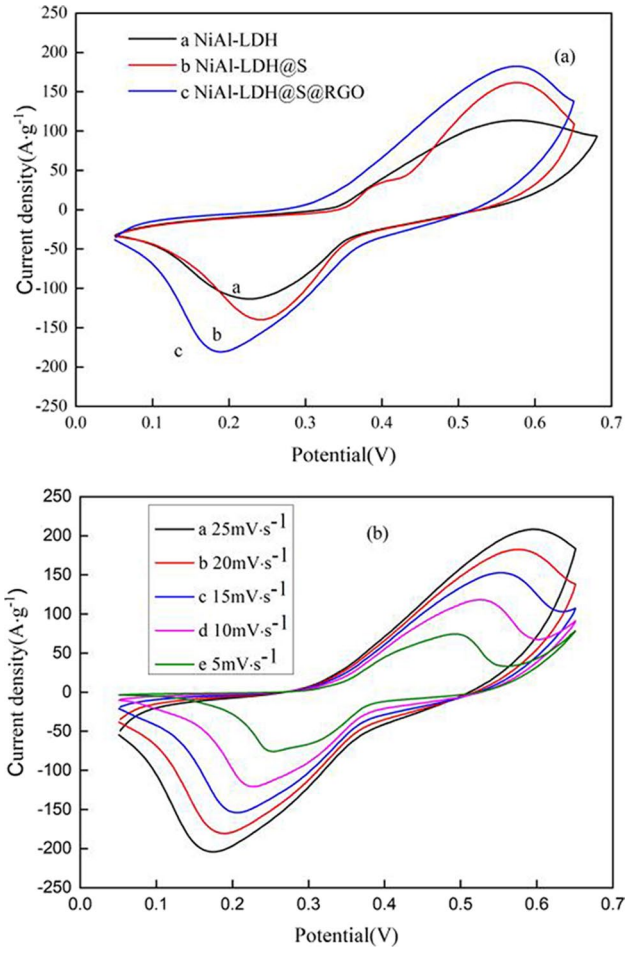

Fig. 6 CV of samples (**a** NiAl-LDH, NiAl-LDH@S, NiAl-LDH@S@RGO; **b** NiAl-LDH@S@RGO)

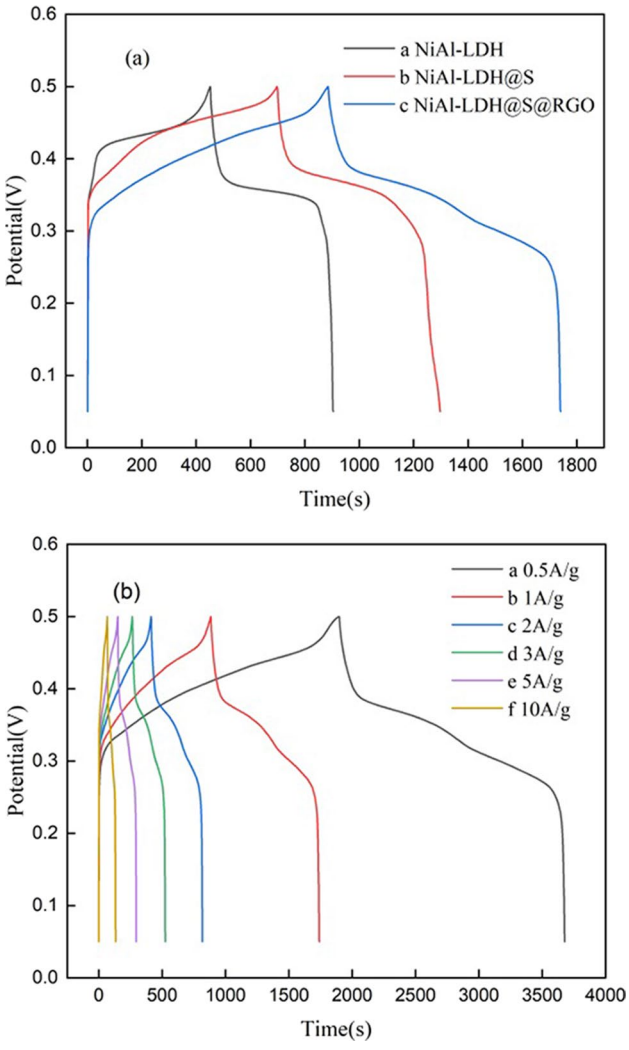

Fig. 7 GCD of samples (**a** NiAl-LDH, NiAl-LDH@S, and NiAl-LDH@S@RGO; **b** NiAl-LDH@S@RGO)

the larger specific surface area of graphene. Because of the rich pore structure and interlayer gaputilizing of NiAl-LDH@S@RGO, the penetration of electrolyte ions, active site, and transport of electrolytes was enhanced, and the specific capacitance was greatly improved.

In addition, the electrochemical active surface area (ECSA) is calculated by CV curve, which depends on the scanning rate of the non-faraday potential segment. ECSA is calculated as 22.51 by the following formula: ESCA = C_{dl}/C_s, which also proves that it is beneficial to improve the active area after vulcanization and loading RGO.

Figure 7b shows the GCD curve of NiAl-LDH@S@RGO in the current range of 0.5–10 A. When the current densities are 0.5, 1, 2, 3, 5, and 10 A/g, the discharge time of it is 1777.2 s, 853.2 s, 403.7 s, 258.5 s, 145.9 s, and 65.3 s, respectively; and the specific capacitance is 1974.7 F/g, 1896 F/g, 1794.2 F/g, 1723.3 F/g, 1621.1 F/g, and 1451.1 F/g. It can be concluded that the larger the current density, the shorter the discharge time and the smaller the specific capacity.

Figure 8a is a comparison of the EIS diagrams of NiAl-LDH, NiAl-LDH@S, and NiAl-LDH@S@RGO. It can be seen that it is composed of a semicircle in the low frequency region and a straight line in the high frequency region, indicating that the reaction process is controlled by the charge transfer process and the diffusion process together. The diameter of the semicircle in the high frequency region represents the charge transfer resistance (Rct), which corresponds to the charge transfer rate. The smaller the Rct, the larger the corresponding charge transfer rate. The value of the intersection between the EIS curve and the abscissa represents the solution resistance (Rs). The impedance parameters of samples are listed in Table 1. From Table 1, the NiAl-LDH@S@RGO has the smallest Rct and Rs, which illustrate that the NiAl-LDH@S@RGO exhibits a lowest resistance to charge-transfer.The straight line part in the low frequency region represents the Warburg impedance generated by electrolyte ion diffusion, which is related to the ion diffusion rate. The larger the direct slope, the smaller the corresponding Warburg impedance. As can be seen from Fig. 8a, NiAl-LDH@S@RGO has the lowest Warburg impedance to ion diffusion. In short, the highly conductive NiAl-LDH@S@RGO composite with a larger specific surface provides a faster transfer rate for charge, with higher conductivity and ion diffusivity.

Figure 8b is the cycle curve obtained by NiAl-LDH@S@RGO after 5000 cycles at a current density of 5 $A \cdot g^{-1}$. It can be known that the capacitance still maintains a great stability after 4000 cycles, and the capacitance cycle rate is 69% at the 5000 cycles, which is dropped 31%, compared with that of 4000 cycles. It is probably because the contact between the electrode

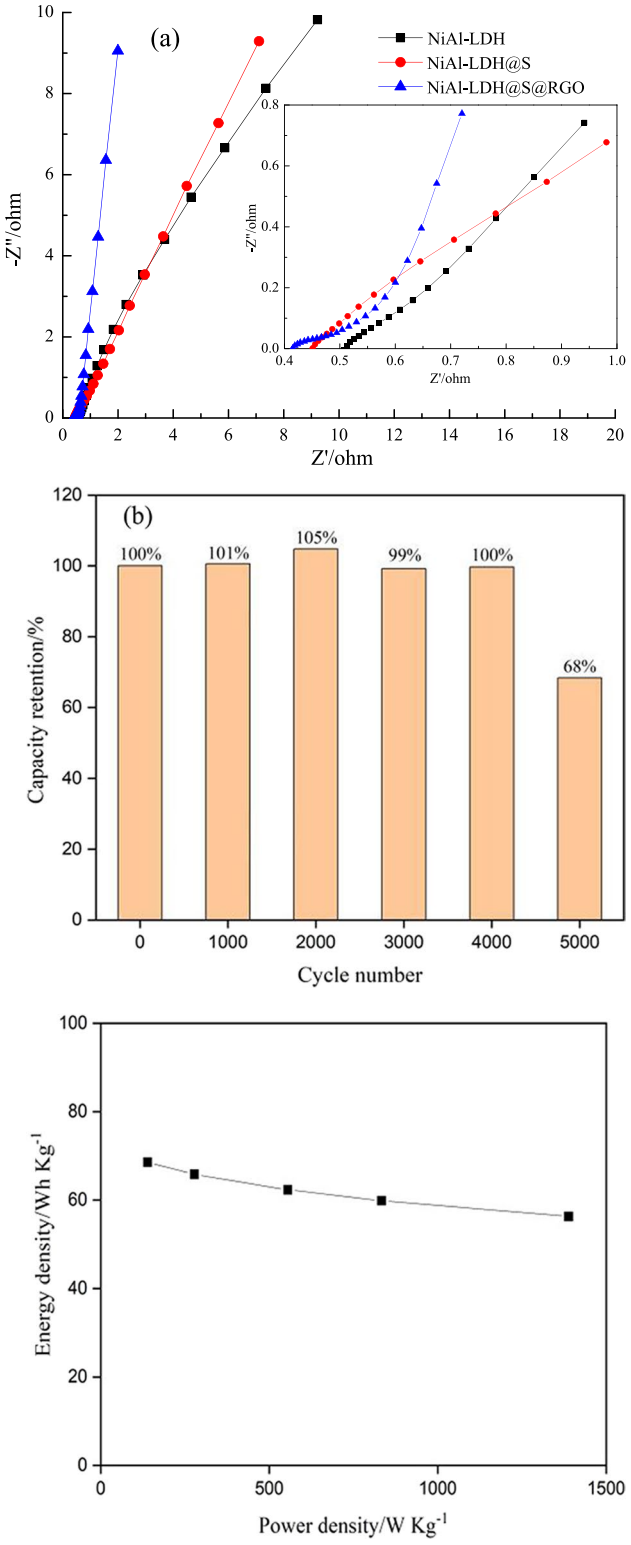

Fig. 8 **a** EIS of the samples NiAl-LDH, NiAl-LDH@S, and NiAl-LDH@S@RGO; **b** capacitance retention of the NiAl-LDH@S@RGO; and **c** Ragone plot of NiAl-LDH@S@RGO

Table 1 Impedance parameters of samples

Samples	Rct/Ω	Rs/Ω
NiAl-LDH	0.43	0.51
NiAl-LDH@S	0.42	0.45
NiAl-LDH@S@RGO	0.30	0.42

material and the electrolyte is gradually insufficient after the long-time EIS cycle test; the capacitance cycle rate began to decline at the 4000 cycles. It indicates that the NiAl-LDH@S@RGO with a longer cycle life can be used as a supercapacitor electrode material. The high cycle performance is mainly attributed to the unique multi-stage structure and rough surface, which in turn improves the utilization rate of the active material and can withstand large structural shrinkage and expansion during the cycle.

As shown in the Ragone plot (Fig. 8c), the energy density of NiAl-LDH@S@RGO can reach as high as 68.5 Wh kg^{-1} at the power density of 138 W kg^{-1} and still maintains a high value of 65.8 Wh kg^{-1} even at a high power density of 277 W kg^{-1}. The high energy density is attributed to the high specific capacitance of the electrodes. These results reveal that the material NiAl-LDH@S@RGO composite could be a good supercapacitor device.

Conclusion

NiAl-bimetal hydroxide@sulfide@graphene (NiAl-LDH@S@RGO) composite was prepared by two-step method, and its electrochemical performance was studied. Compared with the original NiAl-LDH (1000.2 F/g), the specific capacitance value is nearly doubled due to partial vulcanization and loading of graphene. The discharge time reached 853.2 s at a current density of 1 A/g; the specific capacitance was as high as 1896 F/g; and its value also reached 1451.1 F/g at a high current density of 10 A/g. After 5000 cycles, it has a capacitance retention rate of 69%, indicating that the composite material has a better cycle retention rate. These results indicate that sulfurized and loaded graphene significantly improved the electrochemical performance of LDH.

References

1. Wang XW, Sun GZ, Li N, Chen P (2016) Quantum dots derived from two-dimensional materials and their applications for catalysis and energy. Chem Soc Rev 45(8):2239
2. Fan K, Chen H, Ji Y, Huang H, Claesson PM, Daniel Q, Philippe B, Rensmo H, Li F, Luo Y et al (2016) Nickel-vanadium monolayer double hydroxide for efficient electrochemical water oxidation. Nat Commun 7:11981
3. Xu H, Wu J, Liu J, Chen Y, Fan X (2018) Growth of cobalt–nickel layered double hydroxide on nitrogen-doped graphene by simple co-precipitation method for supercapacitor electrodes. J Mater Sci 29(20):17234
4. Qi D, Liu Y, Liu Z, Zhang L, Chen X (2017) Design of architectures and materials in in-plane micro-supercapacitors: current status and future challenges. Adv Mater 29(5):1602802
5. Zardkhoshoui AM, Hosseiny Davarani SS (2018) All-solid-state, flexible, ultrahigh performance supercapacitors based on the Ni-Al LDH-rGO electrodes. J Alloy Compd 750:515
6. Chen J, Li S, Qian K, Lee PS (2018) NiMn layered double hydroxides derived multiphase Mn-doped Ni sulfides with reduced graphene oxide composites as anode materials with superior cycling stability for sodium ion batteries. Mater Today Energy 9:74
7. Song Y, Wang J, Li Z, Guan D, Mann T, Liu Q, Zhang M, Liu L (2012) Self-assembled hierarchical porous layered double hydroxides by solvothermal method and their application for capacitors. Microporous Mesoporous Mater 148(1):159
8. Li Y, Ye K, Cheng K, Yin J, Cao D, Wang G (2015) Electrodeposition of nickel sulfide on graphene-covered make-up cotton as a flexible electrode material for high-performance supercapacitors. J Power Sources 274:943
9. Yu L, Shi N, Liu Q, Wang J, Yang B, Wang B, Yan H, Sun Y, Jing X (2014) Facile synthesis of exfoliated Co-Al LDH-carbon nanotube composites with high performance as supercapacitor electrodes. Phys Chem Chem Phys 16(33):17936
10. Han Y, Liu N, Wang N, He Z, Liu Q (2018) Assembly of Ni-Al layered double hydroxide and oxide graphene quantum dots for supercapacitors. J Mater Res 33(24):4215
11. Wang L, Han Y, Feng X, Zhou J, Qi P, Wang B (2016) Metal-organic frameworks for energy storage: batteries and supercapacitors. Coord Chem Rev 307:361
12. Zheng W, Sun S, Xu Y, Yu R, Li H (2018) Facile synthesis of NiAl-LDH/MnO_2 and NiFe-LDH/MnO_2 composites for high-performance asymmetric supercapacitors. J Alloy Compd 768:240
13. Zhao J, Chen J, Xu S, Shao M, Zhang Q, Wei F, Ma J, Wei M, Evans DG, Duan X (2014) Hierarchical NiMn layered double hydroxide/carbon nanotubes architecture with superb energy density for flexible supercapacitors. Adv Func Mater 24(20):2938
14. Baker CO, Huang X, Nelson W, Kaner RB (2017) Polyaniline nanofibers: broadening applications for conducting polymers. Chem Soc Rev 46(5):1510
15. Hao T, Wang W, Yu D (2018) Hierarchical NiCo layered double hydroxides nanosheets on carbonized CNT/cotton as a high-performance flexible supercapacitor. J Mater Sci 53(20):14485
16. Wang Z, Zhang X, Wang J, Zou L, Liu Z, Hao Z (2013) Preparation and capacitance properties of graphene/NiAl layered double-hydroxide nanocomposite. J Colloid Interface Sci 396:251
17. Yang J, Yu C, Hu C, Wang M, Li S, Huang H, Bustillo K, Han X, Zhao C, Guo W (2018) Surface-confined fabrication of ultrathin nickel cobalt-layered double hydroxide nanosheets for high-performance supercapacitors. Adv Funct Mater 28(44):1803272
18. Cha JH, Park EB, Han SW, Kim YD, Jung DY (2019) Core-shell structured cobalt sulfide/cobalt aluminum hydroxide nanosheet arrays for pseudocapacitor application. Chem Asian J 14(3):446
19. Sun L, Zhang Y, Zhang Y, Si H, Qin W, Zhang Y (2018) Reduced graphene oxide nanosheet modified NiMn-LDH nanoflake arrays for high-performance supercapacitors. Chem Commun (Camb) 54(72):10172
20. Niu YL, Li RY, Li ZJ, Fang YJ, Liu JK (2013) High-performance supercapacitors materials prepared via in situ growth of

NiAl-layered double hydroxide nanoflakes on well-activated graphene nanosheets. Electrochim Acta 94:360
21. Park S, An J, Potts JR, Velamakanni A, Murali S, Ruoff RS (2011) Hydrazine-reduction of graphite- and graphene oxide. Carbon 49(9):3019
22. Li L, Li RM, Gai SL, He F, Yang PP (2014) Facile fabrication and electrochemical performance of flower-like Fe_3O_4@C@layered double hydroxide (LDH) composite. J Mater Chem A 2(23):8758
23. Hanh MB, Paula FG, Tabea G, Merle B, Anne B, Richard F, Normen S, Markus T, Olaf H (2022) 3D printed co-precipitated Ni-Al CO_2 methanation catalysts by binder jetting: fabrication, characterization and test in a single pellet string reactor. Appl Catal A Gen 643:118760
24. Viresh K, Himanshu SP (2021) Miniaturization of binary metal sulfides electrode materials in water-ethanol solvent medium: remarkable improvement in specific capacitance and cyclic stability. Mater Chem Phys 272:125042